

The structure of Fe(III) ions in strongly alkaline aqueous solutions from EXAFS and Mössbauer spectroscopy†

Pál Sipos,^{*a} Dalma Zeller,^a Ernő Kuzmann,^b Attila Vértes,^b Zoltán Homonnay,^b Monika Walczak^c and Sophie E. Canton^c

Received 24th April 2008, Accepted 30th June 2008

First published as an Advance Article on the web 27th August 2008

DOI: 10.1039/b806937a

To establish the structure of ferric ions in strongly alkaline (pH > 13) environments, aqueous NaOH solutions supersaturated with respect to Fe(III) and the solid ferric-hydroxo complex salts precipitating from them have been characterized with a variety of experimental techniques. From UV measurements, in solutions of pH > 13, only one kind of Fe(III)-hydroxo complex species was found to be present. The micro crystals obtained from such solutions were proven to be a new, so far unidentified solid phase. Mössbauer spectra of the quick-frozen solution and that of the complex salt indicated a highly symmetrical ferric environment in both systems. From the EXAFS and XANES spectra, the environment of the ferric ion in these solutions (both native and quick-frozen) and in the complex salt was found to be different. In the complex salt, the bond lengths are consistent with an octahedral coordination around the ferric centres. In solution, the coordination geometry of Fe(III) is most probably tetrahedral. Our results demonstrate that in strongly alkaline aqueous solutions, ferric ions behave very similarly to other structurally related trivalent ions, like Al(III) or Ga(III).

Introduction

The study of structural aspects of trivalent hard metal ions hydrolysis, such as Fe(III), Al(III) or Ga(III), is a classical theme in inorganic coordination chemistry^{1–4} and the topic has considerable commercial importance. For example, technologies used by the hydrometallurgical industry (where hydrolytic processes are invariably involved and in some cases dominate the process chemistry) require such knowledge on a daily basis. The fundamental question of whether these trivalent metal ions are four- or six-fold coordinated in the hydroxo complex(es) formed in strongly alkaline aqueous solutions, is still intensely investigated today. For example, from Raman,^{4,5} solution X-ray diffraction⁶ and EXAFS⁷ measurements it has been established that Al(III) and Ga(III) are predominantly four-fold coordinated even at the highest concentrations of base. ²⁷Al and ⁷¹Ga NMR measurements support these findings as the observed variations in the NMR patterns were fully accounted for in terms of the formation of contact ion-pairs,^{5,8} without the need to invoke even the existence of a six-fold coordinated species.

The identity and structure of the water soluble Fe(III)-hydroxo complexes forming in strongly alkaline solutions is more unclear and controversial. The well known book of Baes and Mesmer⁹ states that the only water soluble mononuclear ferric hydroxo complex at pH ≤ 13 is the tetrahedral [Fe(OH)₄][−]. This has

been supported by a large number of observations.^{10–14} For example, from the UV-spectroscopic measurements, besides an unspecified polynuclear ferric-hydroxo complex, the formation of [Fe(OH)₄][−] was deduced.^{10,11} Solubility measurements also strongly support that [Fe(OH)₄][−] is the last member of the stepwise Fe(III)-hydroxo complexes.^{12–14} However, Cotton and Wilkinson¹⁵ mention the possible formation of [Fe(OH)₆]^{3−} in strong base solutions. In a recent paper, from a large number of accurate UV-vis spectroscopic measurements, Perera and Hefter¹⁶ reported the consecutive formation of [Fe(OH)₅]^{2−} and [Fe(OH)₆]^{3−} as well as [Fe(OH)₄][−] with the exclusive presence of [Fe(OH)₆]^{3−} at pH ≥ 13. As far as solid ferric hydroxo complexes are concerned, some naturally occurring minerals^{17–19} are proven to consist of [Fe(OH)₆]^{3−} structural building blocks and various salts containing [Fe(OH)₆]^{3−}, [Fe(OH)₇]^{4−} and [Fe(OH)₈]^{5−} synthesized under laboratory conditions and have been described both in the literature^{20–22} and in university textbooks.²³ Moreover, to the best of our knowledge, solid state complex salts consisting of [Fe(OH)₄][−] units have not been prepared and characterized (see below). It is to be noted here, that the relationship between the chemical species observed in a given solution, and the structure of the solid complex salt crystallizing from it, is not straightforward. For example, a number of solid complexes either with [M(OH)₄][−] or with [M(OH)₆]^{3−} (M = Al(III) and Ga(III)) building blocks are known from the literature,^{24–26} but in the solutions from which these complexes are obtained, neither [Al(OH)₆]^{3−} nor [Ga(OH)₆]^{3−} are present in experimentally detectable quantities.^{5,8}

Kamnev *et al.* made a remarkable effort^{27–29} to elucidate the Mössbauer spectrum of the Fe(III)-hydroxo complex species forming in strongly alkaline aqueous solutions. In concentrated (15–17 M) NaOH solution, ferric ions were found to form a reddish-orange (supposedly colloidal and/or polynuclear) compound. When the solvent was evaporated, the colour of the complex

^aUniversity of Szeged, Department of Inorganic and Analytical Chemistry, PO Box 440, H-6701, Szeged, Hungary. E-mail: sipos@chem.u-szeged.hu

^bMTA-ELTE Research Group on the Application of Nuclear Techniques in Structural Chemistry, Roland Eötvös University Pázmány Péter Sétány 1/A, H-1117, Budapest, Hungary

^cChemical Physics Department, Chemical Centre, Lund University, PO Box 124, SE-22100, Lund, Sweden

† Electronic supplementary information (ESI) available: PXRD and derivative XANES spectra. See DOI: 10.1039/b806937a

disappeared. The singlet in the Mössbauer spectrum of the solid obtained (isomer shift is $0.68 \pm 0.02 \text{ mm s}^{-1}$ and 0.72 mm s^{-1} half width) indicated the presence of a 'symmetrically coordinated mononuclear hydroxo complex, statistically distributed in the $\text{NaOH}\cdot\text{H}_2\text{O}$ matrix'.²⁷ Upon heating, the symmetry of the complex was retained and the observed increase in the line width was attributed to the non-uniformity of the complexes' environment due to non-uniform drying.²⁸ The colloidal and/or polynuclear complex (during a 3.5 years ageing period) was found to transform to a reddish-brown solid complex with Mössbauer spectral parameters very similar to those of the solid obtained upon evaporation.²⁹ From this, Kamnev *et al.* concluded that (in accordance with their UV-vis observations^{10,11} obtained for solutions) the species responsible for the unique Mössbauer spectrum is most likely to be built up from $[\text{Fe}(\text{OH})_4]^-$ units in the solid state. This explanation is, however, not unequivocal for several counts. Firstly, the presence of $[\text{Fe}(\text{OH})_4]^-$ both in solution and in the solid state has not been supported by direct structural information (*i.e.*, by using techniques providing data for the coordination number and bond lengths). Secondly, $[\text{Fe}(\text{OH})_6]^{3-}$ is also of high symmetry, and from a species like this, very low quadrupole splitting would be expected, similar to that of $[\text{Fe}(\text{OH})_4]^-$, therefore for the Mössbauer spectroscopy the two micro-environments are indistinguishable. Thirdly, proving the direct correspondence, between the complex structures existing in solution and in the solid state, would require further experimental observations.

The aim of the current paper is to elucidate the structure of ferric ions in aqueous solutions of $\text{pH} > 13$. For this, we will describe the preparation of strongly alkaline aqueous solutions with relatively high concentrations of dissolved Fe(III), characterize the local structure of Fe(III) in these solutions (native and quick-frozen state) *via* Mössbauer and EXAFS/XANES spectroscopies, describe the isolation and chemistry of the solid ferric-hydroxo complex salts precipitating from such solutions and compare the structure of Fe(III) in the solutions and also the solid state.

Experimental

Materials

Concentrated NaOH (~20 M) and KOH (~12 M) stock solutions were prepared from Millipore MilliQ water and a.r. (analytical reagent) grade NaOH (Hungharopharma, 99% purity) and KOH (Reanal, a.r. grade), respectively. Their carbonate content was minimized as described previously.³⁰ The density of the solution was determined picnometrically. The exact concentration of the stock solution was determined by acid–base titration, following an accurate gravimetric dilution of the base solution. For the titration, HCl solution ('Convol' volumetric standard, accuracy $\pm 0.1\%$) and phenolphthalein indicator was used. The NaOH solution was stored in an airtight, caustic resistant Pyrex bottle.

Ferric stock solutions ($[\text{FeCl}_3]_{\text{T}} \sim 0.5 \text{ M}$, $[\text{HCl}]_{\text{T}} \sim 2.5 \text{ M}$, where the subscript T denotes analytical or total concentration) were prepared from $\text{FeCl}_3\cdot 6\text{H}_2\text{O}$ (Reanal, a.r. grade) and concentrated HCl (*ca.* 37 wt%, Merck, a.r. grade). The exact concentration of the solution was determined by EDTA titration. $\text{Fe}(\text{ClO}_4)_3$ solutions were made of solid $\text{Fe}(\text{ClO}_4)_3\cdot 12\text{H}_2\text{O}$ (prepared and kindly donated by Dr A. Szorcik) and $\text{HClO}_{4\text{cc}}$ (*ca.* 30 wt%, Merck, a.r. grade). Freshly prepared ferric-oxy-hydroxide (for

which, as a practical shorthand, FeOOH will be used hereafter) was obtained from a diluted FeCl_3 solution (100 mL, 1 mM) precipitated with an excess of NaOH (~0.1 M, 5 mL added dropwise during vigorous stirring). The precipitate was collected on a filter paper and washed with distilled water, until the conductivity of the filtrate decreased to a value similar to that of the distilled water. The precipitate was used for further syntheses within one hour. All the other chemicals were of analytical grade.

Methods

UV-vis spectra. The UV-vis spectra of Fe(III)-containing alkaline solutions were recorded in the $200 \text{ nm} < \lambda < 800 \text{ nm}$ wavelength range on a Hewlett-Packard diode array spectrophotometer, using a 1 mm and a 10 mm quartz cuvette. Blank solutions were prepared for each individual sample and were subtracted from the spectra in question. The cuvette was stored in $\text{KMnO}_4\text{--H}_2\text{SO}_4$ solution to remove impurities, and was cleaned with a $\text{HNO}_3\text{--H}_2\text{O}_2$ mixture and distilled water prior to the experiments. **Caution!** Both mixtures are of an explosive nature, and special attention has to be taken to observe the work safety regulations during their use.

Elemental analyses. The Na^+ and Fe^{3+} content of the solid ferric-hydroxo complex salts were determined by flame photometry and by permanganometric titration, using the Zimmermann–Reinhardt method, respectively. For the flame photometric measurements, a PFP7-type instrument was used. A calibration series in the range of 0–10 ppm (linear instrument response range) was prepared by accurate dilution of a NaCl primary standard solution. The flame photometer was calibrated before and after the measurement with three independently prepared parallels for each sample. The corrections for the matrix effect caused by the constituents of the samples other than sodium were considered to be unnecessary.

pH-metric titrations. The presence of a carbonate impurity in the solid ferric-hydroxo complex salts was checked by pH-metric titration. The instrumentation has been described in detail elsewhere.³¹ During the measurement, an accurately weighed portion (50–100 mg) of the sample was suspended in a $I = 0.1 \text{ M}$ NaClO_4 supporting electrolyte and was titrated with standardized ~0.1 M HClO_4 solution in an inert atmosphere (Ar).

Thermogravimetric analyses. (TG and DTG) measurements were performed using a MOM Derivatograph Q-1500D instrument, using a 2.5 and a $10 \text{ }^\circ\text{C min}^{-1}$ heating rate.

IR and Raman spectra. Mid and far IR measurements on the solid complexes and reference materials (Na_2CO_3 and NaOH) were performed using a FTS 65/A896 BioRad Digilab Division spectrometer equipped with a Mtech 200 type photoacoustic detector. The Raman spectra were measured with a BioRad Dedicated Raman spectrometer using a Spectrophysics T10-106C Nd:YVO₄ laser operating at 1064 nm and a germanium detector cooled with liquid nitrogen. For both the Raman and the IR spectra, 1024 scans at a 4 cm^{-1} resolution were used.

Powder X-ray diffraction. XRD patterns of the solid samples and some of the reference compounds (Na_2CO_3 and NaOH) were recorded in the $2\theta = 2\text{--}50^\circ$ range using a Philips PW1710 instrument, employing $\text{Cu K}\alpha$ radiation.

Mössbauer spectroscopy. ^{57}Fe Mössbauer spectra of the salts and the frozen solutions were recorded with conventional Mössbauer spectrometers (Wissel and Ranger) in a transmission geometry at 300 and 80 K in a bath-type cryostat. The solution samples were quenched in the form of drops in a copper container situated on an aluminium slab almost completely immersed in liquid nitrogen. This freezing technique is expected to provide a cooling rate, which is safely over the critical cooling rate necessary to preserve the original structure of the solution in the liquid state. However, for the samples, where precipitation had already commenced before quick-freezing (*e.g.*, for the heavily supersaturated solutions studied in this work), only the fraction, which is truly in solution can be considered as the one with the original structure. Isomer shifts are given relative to α -iron. A $^{57}\text{Co}/\text{Rh}$ γ -radiation source of 3×10^9 Bq activity was used. The Mössbauer spectra were analyzed by least-squares fitting of the Lorentzian lines with the help of the MOSSWINN program.³²

XANES and EXAFS spectroscopy. The Iron K edge (7112 eV) XANES and EXAFS spectra were measured on beamline I811 at the MAXlab facility, Lund, Sweden.³³ This is a superconducting multipole wiggler beamline equipped with a water cooled channel cut Si(111) monochromator delivering at 10 keV, approximately 2×10^{15} photons s^{-1} (0.1% bandwidth) with horizontal and vertical FWHM of 7 and 0.3 mrad. A beamsize of 0.5 mm \times 1.0 mm (width \times height) was used. The incident beam intensity I_0 was measured with an ionization chamber filled with a mixture of He–N₂. The data were measured in transmission mode for the crystalline samples and in fluorescence mode for the solution and quick-frozen samples, respectively. The cell-to-detector distance was varied with concentration in order to avoid detector saturation.

Results and discussion

UV spectra of caustic ferric solutions

The solubility of ferric-oxides or oxy-hydroxides in alkaline solutions under ambient conditions is estimated to be in the range of 10^{-5} – 10^{-6} M.¹⁴ When FeCl_3 solution is added to a $[\text{NaOH}]_{\text{T}} \geq 1$ M solution, various forms of Fe-oxy-hydroxides (*e.g.*, amorphous ferric-hydroxide, ferric-hydrate or more often goethite³⁴) are precipitated and only a small fraction of the ferric ions remain dissolved in the solution. To a NaOH solution series ($1 \text{ M} \leq [\text{NaOH}]_{\text{T}} \leq 20 \text{ M}$) an FeCl_3 solution was added until precipitate formation (*i.e.*, $[\text{FeCl}_3]_{\text{T}} \geq 1 \text{ mM}$) and the solutions were vigorously stirred for a couple of weeks. The precipitates were separated from the solutions *via* filtration (using a unit specifically designed to filtrate strong caustic solutions, consisting of a polysulfonate made Nalgene vacuum filter equipped with a Versapor membrane filter with a pore size of 0.45 μm). The filtrates were found to be invariably colourless, indicating that the coloured complexes observed in similar solutions by Kamnev *et al.*^{10,11} may have been due to colloidal and not to dissolved iron-containing species. The UV spectra of the filtrates were recorded and no significant baseline shifts were observed, suggesting that practically all the colloidal precipitate was removed *via* filtration. A shoulder in the range of $\lambda = 250$ – 300 nm was observed for each solution (the region at $\lambda < 250$ nm is masked by the intense absorption of NaOH³⁵). This feature is generally thought to be associated with ferric ions in caustic solutions³⁵ and is very similar

to the spectrum described in ref. 16, recorded for ferric containing solutions at $\text{pH} > 13$. In this work¹⁶ this shoulder was suggested to correspond to the $[\text{Fe}(\text{OH})_6]^{3-}$ species.

On the basis of our measurements, the intensity of this shoulder, as expected, increases with increasing $[\text{NaOH}]_{\text{T}}$, corresponding to *ca.* ten-fold increase in $[\text{Fe}(\text{III})]_{\text{T}}$ within the series. After background subtraction and normalization, the spectra obtained are perfectly superimposable (Fig. 1). From the $[\text{NaOH}]_{\text{T}}$ and $[\text{Fe}(\text{III})]_{\text{T}}$ independence of the spectra, in solutions of $[\text{NaOH}]_{\text{T}} \geq 1 \text{ M}$ there is no speciation change with the increasing caustic concentrations. Furthermore, there is only one ferric-hydroxo complex species present. As the formation of the polynuclear hydroxo complex species can also be excluded, this sole species is either $[\text{Fe}(\text{OH})_4]^{-}$ ^{9–14} or $[\text{Fe}(\text{OH})_6]^{3-}$.^{15,16}

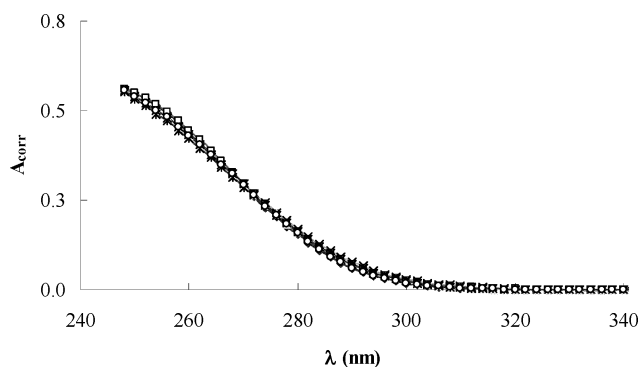


Fig. 1 Background corrected and normalized absorbances as a function of the wavelength for aqueous NaOH solutions (8 solutions in the range of $1 \text{ M} \leq [\text{NaOH}]_{\text{T}} \leq 20 \text{ M}$) saturated with $\text{Fe}(\text{III})$.

Preparation and analysis of the solid ferric-hydroxo complex salt

After several weeks of rest, an off-white solid precipitated from the ferric-containing $[\text{NaOH}]_{\text{T}} = 20 \text{ M}$ solution used for recording the UV spectra. When the solid was separated from the mother liquor, it turned brown immediately due to exposure to air moisture, suggesting, that it contained some $\text{Fe}(\text{III})$. The experiment was repeated several times, and the experimental parameters were systematically changed, in order to achieve a synthesis method for producing a sufficiently large amount of this solid substance with a well-defined composition. The largest yield was achieved, when 20 mL FeCl_3 solution (0.1 M) was added dropwise (*i.e.*, 0.2 mL portions) to 200 mL of hot (80 – 100 $^{\circ}\text{C}$), vigorously stirred NaOH solution ($\sim 20 \text{ M}$). The vast majority of the initially formed reddish-brown precipitate instantaneously dissolved and an apparent ferric concentration of up to 10 mM (several orders of magnitude larger, than the equilibrium solubility of $\text{Fe}(\text{III})$ under these conditions) was attained. The filtration of the hot solution resulted in a colourless filtrate. The solution thus obtained was surprisingly stable. An off-white-to-pale green solid appeared in the resting solution usually after a couple of days. Upon shaking, stirring or when in contact with a rough surface was found to significantly speed up the formation of these crystals. The precipitate/crystals thus formed were very quickly filtered until air-dry and rapidly transferred to a vacuum desiccator (drying material: P_2O_5). During the systematic optimization experiments, the following observations were made:

1. Adding an amount of NaCl to the solution, equivalent to the saline formed during the reaction with the FeCl₃ added, no precipitation was observed. Therefore, the precipitate is not expected to contain significant amounts of NaCl.

2. When the reaction was repeated with a Fe(ClO₄)₃ solution or freshly precipitated, amorphous FeOOH instead of FeCl₃, the formation of the compound was again observed as before, indicating that the phenomenon is largely independent of the anion accompanying the ferric ion.

3. When the reaction was performed by using a saturated (~12 M) KOH solution or solutions with [NaOH]_T < 18 M, practically all the ferric ions precipitated in the form of a reddish-brown gel, and after filtration no precipitation from the colourless mother liquor could be separated.

For the solid compound obtained from five parallel optimized syntheses, variable Na (26–34 wt%) and Fe(III) contents (7.8–10.8 wt%) were found, corresponding to Fe : Na molar ratios of 1 : 7.6–9.6. We observed that the visibly more crystalline pale green specimens had a larger iron concentration, than those with less well-defined (*i.e.*, off-white) colour. From this, we concluded, that the slightly variable colour of the solid products is most likely to be associated with the inevitable residuals of the mother liquor, (which is an almost saturated aqueous solution of NaOH with some NaCl). If not otherwise stated, the pale green microcrystalline sample most likely to contain the least mother liquor residuals was used for further studies. The elemental analysis data for these specimens obtained from two independent syntheses: Fe 10.67 ± 0.07 wt% and Na 34.07 ± 0.08. Fe : Na molar ratio: 1 : 7.66.

The carbonate content of the samples from pH-metric titrations were found to be ≤ 2 mol% of the NaOH. This is consistent with some carbonate impurities formed during the short air exposures of the samples during the manipulations. Therefore, carbonate is unlikely to be an integral component of the sample.

From the TG/DTG measurements (one representative experimental curve is shown in Fig. 2) the compound loses water in two consecutive, slightly overlapping steps. The first (between 100–200 °C) is likely to correspond to crystalline water (as the contribution of adsorbed water is unlikely) and constitutes *ca.* 22 wt% of the total sample mass. The second weight loss (between 200–300 °C) is also likely to be water related, and most probably corresponds to the decomposition of the Na_x[Fe(OH)_{3+x}] units to

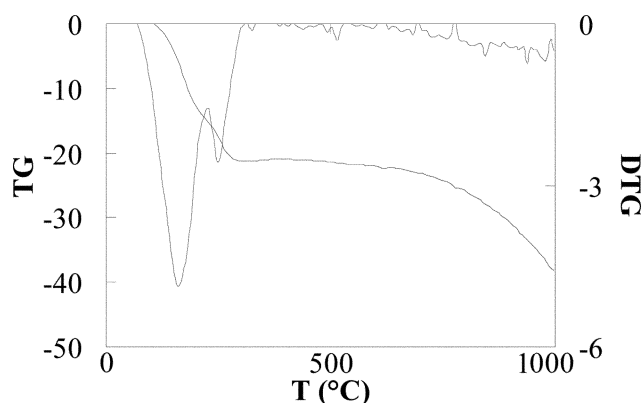


Fig. 2 TG/DTG curves of the solid ferric-hydroxo complex salt, obtained at a heating rate of 10 °C min⁻¹.

FeOOH or Fe₂O₃ and NaOH. A constant mass is attained from 300 °C, and from 800 °C the gradual dehydration of NaOH starts.

XRD patterns of the samples prepared indicated an appreciable crystallinity with well-defined XRD patterns (see Figure S1 in the ESI†). The XRD patterns of the pale green and off-white samples were found to be perfectly superimposable. This means, that the crystalline phase in the various samples is identical and the variation in the colour is associated with the varying amount of residual NaOH, which is present in the samples in an X-ray amorphous form.

From the XRD, a significant amount of crystalline Na₂CO₃ is also unlikely to be present, consistent with the results of the pH-metric titrations. The XRD patterns obtained did not match any of those registered in the JCPD database, this is another indication that our sample is not a physical mixture of the constituents and it might be a solid phase not so far described.

From the data described in this section, the powder obtained is a solid Na salt of an anionic Fe-hydroxo complex, embedded in an amorphous NaOH matrix. It can be described with the general formula of Na_x[Fe(OH)_{3+x}]_yNaOH·zH₂O.

A comparison of the Raman and the far-IR spectra of the same specimen (in particular, the comparison of the peaks in the M–O stretching range, *i.e.*, between 300–550 cm⁻¹), in principle, enables us to distinguish between tetrahedral and octahedral environments around the metal ion.³⁶ For the ferric-hydroxo complex salt, a relatively well-defined Raman spectrum with a well-defined peak at ~490 cm⁻¹ and a broad feature at ~340 cm⁻¹ has been obtained. However, the IR spectrum recorded turned out to be featureless, with no peaks that are clearly distinguishable from the baseline noise. This prohibited the determination of the coordination geometry of Fe(III) from IR and Raman measurements.

Mössbauer spectra of the solid ferric-hydroxo complex salt and the quick-frozen solution from which it was obtained

The Mössbauer spectra of the solid ferric-hydroxo complex salt were recorded at room temperature (~20 °C) and at liquid N₂ temperature (-193 °C) (Fig. 3 and Table 1). To compare the solution and solid structure of Fe(III) in an alkaline environment, the Mössbauer spectra of quick-frozen solutions from which the solid ferric-hydroxo complex salts can be obtained were also recorded. During the solution preparation, 3.6 mg of ⁵⁷Fe₂O₃ was first completely dissolved in 1 mL of hot HCl_{cc} (~1 M). The solution was evaporated to obtain *ca.* 0.1 mL volume and it was added dropwise to 5 mL of hot NaOH solution (~20 M). When the dissolution was complete, the heating was turned off. The solution was placed in a syringe and quickly transferred to a copper container, situated in liquid N₂. This treatment provided an approximate freezing rate of ≥8 K s⁻¹ and ensures that the solutions' structure is retained in the frozen state. Two preparations were made. During the first preparation (resulting in quick-frozen solution 1 in Table 1 and Fig. 3) the solution was immediately quick-frozen after the complete dissolution of Fe(III) ions. During the second preparation (yielding quick-frozen solution 2 in Table 1 and Fig. 3), sufficient time was allowed to start the precipitation of the ferric-hydroxo complex salt, and a seemingly non-homogeneous solution was quick-frozen.

On the basis of the Mössbauer spectra, the solid product formed has a highly symmetrical geometric structure, which could

Table 1 Mössbauer spectral parameters (IS: isomer shift, QS: quadrupole splitting) for various samples containing ferric species at various temperatures

Sample	$T/^{\circ}\text{C}$	IS ^a /mm s ⁻¹	QS ^b /mm s ⁻¹	Line width/mm s ⁻¹
Ferric-hydroxo complex salt	20	0.310	0.289	0.73
	-193	0.409	0.310	0.80
Quick-frozen solution 1 ^c	-193	0.462	0.444	0.65
Quick-frozen solution 2 ^d	-193	0.458	0.367	0.71
Fe(III)-complex in a NaOH matrix ²⁷	-193	0.68 ^e	—	0.72
Heat-treated [Fe(OH) ₄] ⁻ in a NaOH matrix ²⁸	-193	0.62	—	0.79
Reddish-orange [Fe(OH) ₄] ⁻ from solution ²⁹	-193	0.62	—	0.59

^a Estimated standard deviation ± 0.010 mm s⁻¹. ^b Estimated standard deviation ± 0.020 mm s⁻¹. ^c Quick-freezing performed immediately after complete dissolution of Fe(III) in ~ 20 M caustic; the data relate to the broad central singlet; the description of the sextet can be found in the text. ^d Quick-freezing performed when the solid ferric-hydroxo complex salt had already started to precipitate from a solution identical to that used for preparing quick-frozen solution 1. ^e Identical IS value is reported for room temperature measurements in ref. 27.

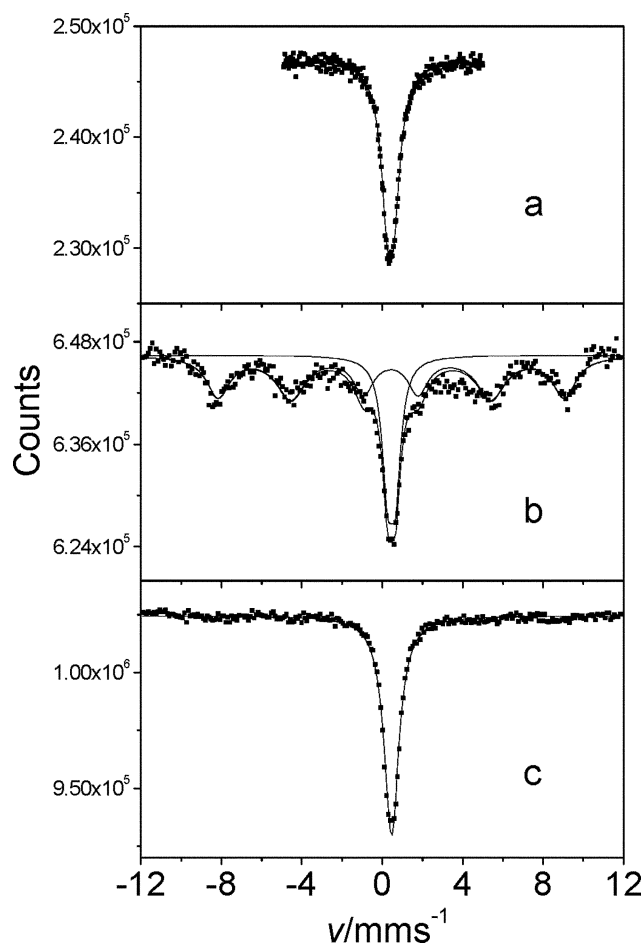


Fig. 3 Mössbauer spectra of the ferric-hydroxo complex salt (upper spectrum) and that of the quick-frozen solution from which solid ferric-hydroxo complex salts are obtained (middle and lower spectra). Middle spectrum: quick-freezing was performed immediately after complete dissolution of ⁵⁷Fe(III) in ~ 20 M caustic. Lower spectrum: quick-freezing was performed when the solid ferric-hydroxo complex salt had already started to precipitate from the same solution.

be both octahedral and tetrahedral. (Note, that the Mössbauer trace characteristic to the solid product was also observed in quick-frozen solution 1, most probably due to the onset of its crystallization prior to the commencement of rapid cooling. This is not really surprising, as preparative work was performed under

micro-conditions and the heavily supersaturated solution was subjected to a range of transfer procedures, which facilitated the onset of crystal formation). The Mössbauer parameters of the solid sample are similar to those published by Chappert *et al.*³⁷ In this publication a $3d^{5.70}4s^{0.169}$ electronic structure was calculated for iron(III) in the FeO_6^{-9} environment. However, Kamnev *et al.* claimed,^{10,11,27-29} that such Mössbauer traces correspond to tetrahedral $[\text{Fe}(\text{OH})_4]^-$ complexes. Thus, the central paramagnetic part of the Mössbauer spectrum represents the small (super-paramagnetic) particles of $[\text{Fe}(\text{OH})_4]^-$ or $[\text{Fe}(\text{OH})_6]^{3-}$ with particle sizes less than $\sim 6\text{--}8$ nm.^{38,39}

It is interesting to note that the Mössbauer spectrum of quick-frozen solution 1 contained a magnetic sextet (with 53.34 T effective magnetic field) as well. The appearance of this component can be explained by the slow paramagnetic spin relaxation due to the low concentration, which results in a weak spin–spin interaction (a slow spin flip–flop) and to the low temperature, which results in a weak spin–lattice interaction.

The Mössbauer spectra of samples containing paramagnetic iron(III) can show magnetic splitting if the average time of their paramagnetic spin relaxation (τ_{PSR}) is longer than the average time of Larmor precession of the magnetic moment of the atomic nucleus (τ_{L}). If the concentration of iron(III) species in the solution and the actual temperature are low (< 0.05 M and < 100 K, respectively) the spin–spin and spin–lattice interactions are weak and the average times of spin–spin (τ_{SSR}) and spin–lattice (τ_{SLR}) relaxations will be long.^{38,39} Consequently, τ_{PSR} , which reads

$$\tau_{\text{PSR}} = \frac{1}{\frac{1}{\tau_{\text{SSR}}} + \frac{1}{\tau_{\text{SLR}}}}$$

will be longer than τ_{L} . Under these conditions, the Mössbauer spectra show magnetic structure.

On the basis of the Mössbauer spectra, we can suppose that the freshly prepared solution contains both mononuclear and super-paramagnetic particles and the aged solution has no more mononuclear iron(III) species. (Note, that in the case of mononuclear iron(III) containing units, the iron ions are far apart from each other and this results in a weak spin–spin interaction, a slow paramagnetic spin relaxation and consequently, magnetic splitting. In the super-paramagnetic particles we have an opposite situation; iron(III) ions will be close to each other, the spin–spin

interaction will be stronger, the paramagnetic spin relaxation will be faster and the magnetic structure disappears.)

XANES and EXAFS spectra of the solid ferric-hydroxo complex salt and the solution (both native and quick-frozen) from which it was obtained

To compare the local structure of Fe(III) in the different states, several XANES and EXAFS spectra of the crystalline solid ferric-hydroxo complex salt and the solution were recorded. A 20 M NaOH solution heavily supersaturated with ferric ions ($[\text{Fe(III)}]_{\text{T}} \sim 10 \text{ mM}$), was prepared and investigated. Given that such solutions are prone to decompose (yielding the solid ferric-hydroxo complex salt), only the XANES spectrum could be recorded. Since no precipitation occurred during the 15 min long measurement, the structural information extracted from the XANES spectrum is that of the ferric ions in solution. (Note, that for the EXAFS measurements, a sufficiently larger volume of sample was prepared, than for the Mössbauer measurements. Therefore, the lack of precipitate in the former could readily be checked. This was not that straightforward for the samples prepared on microscale for the Mössbauer experiments.)

For the XANES/EXAFS measurements, 10 mL FeCl_3 solution ($\sim 0.1 \text{ M}$) was added dropwise (*i.e.*, 0.2 mL portions) to a 100 mL, hot ($80\text{--}100 \text{ }^\circ\text{C}$), vigorously stirred NaOH solution ($\sim 20 \text{ M}$). The hot solution was filtrated and in the colourless filtrate the ferric concentration was *ca.* 9 mM. A fraction of the supersaturated solution was quickly transferred to a custom made Teflon sample holder *via* a piston pipette, was quick-frozen in liquid N_2 and the EXAFS spectrum was recorded. Providing that the local structure of ferric ions is retained during quick-freezing, the structure of Fe(III) in solution could be deduced from the EXAFS analysis.

XANES spectra. The XANES spectra of the three samples investigated are shown in Fig. 4. The qualitative characteristics (*i.e.*, positions and intensities) of the XANES region are sensitive to the coordination geometry, oxidation state of the absorbing atom and to the chemical identity of the surrounding ligands.^{40,41} The Fe K edge spectrum of the ferric ion is known to consist

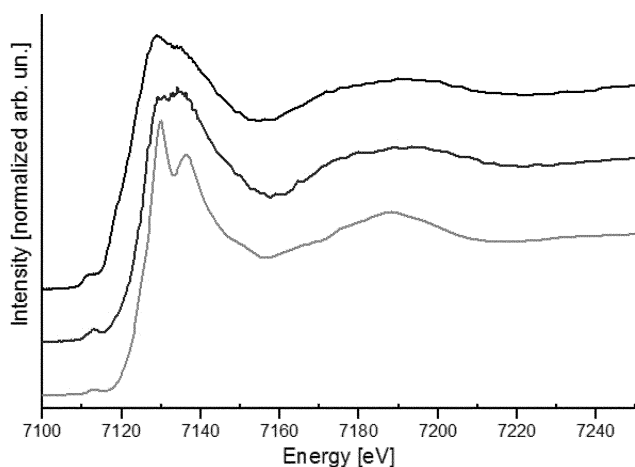


Fig. 4 XANES spectra of the solid ferric-hydroxo complex salt (lower spectrum), the strongly alkaline ($[\text{NaOH}]_{\text{T}} = 20 \text{ M}$) solution supersaturated with ferric ions (middle spectrum) and the same supersaturated solution after quick-freezing (upper spectrum).

of three features: a pre-edge peak at $7113\text{--}7113.7 \text{ eV}$ ($1s \rightarrow 3d$ transition), a broad maximum or shoulder in $7122\text{--}7123.3 \text{ eV}$ ($1s \rightarrow 4s$ transition) and an edge crest at $7128.8\text{--}7132.1 \text{ eV}$ ($1s \rightarrow 4p$ transition).^{42–44}

For complexes in a centrosymmetric (*e.g.*, octahedral) environment, the $1s \rightarrow 3d$ transition is an electric dipole forbidden transition by parity considerations.⁴⁵ For example, both for the metallic iron and for the $[\text{Fe}(\text{CN})_6]^{3-}$, no low energy absorption was observed.⁴⁶ The small intensity that is nevertheless reported for certain compounds with an octahedral environment, can be attributed to vibronically allowed transitions⁴⁷ or to an electric quadrupole coupling.⁴⁵

For complexes in a non-centrosymmetric (*e.g.*, tetrahedral) environment, mixing of the 3d to the dipole allowed 4p in the molecular orbital along the distortion provides oscillator strength to the transition from a Fe 1s orbital. The role of ligand orbitals is considerably smaller than that of the 1s and 4p because of the exponential decay of the atomic orbitals on the two separated atoms.

The total pre-edge intensities of the octahedral high-spin ferric complexes range from 4–7.3, with an average intensity of 4.9 and increases with decreasing coordination number for the model complexes, reflecting the loss of symmetry inversion.⁴¹ It was found to vary inversely with coordination number, 8 units for 6-coordinated, 16 units for 5-coordinated and 24 units for 4-coordinated.⁴⁷

In the samples studied, the areas of the pre-edge peaks of the $1s \rightarrow 3d$ transition were calculated from the position of the inflection point, (which gives the photon energy necessary to excite a K electron into the first empty level of the Fermi distribution). The background function was determined by a least-squares fit of an arctangent (initial absorption close to threshold) and a first order polynomial below the inflection point. The edge jump was obtained by fitting a first order polynomial. The difference between these 2 lines at the inflection point was used as the normalization factor for the pre-edge peak.

Based on the direct comparison of the line intensities, the coordination number of the ferric ions is smaller in the solution and in the quick-frozen solution than in the solid ferric-hydroxo complex salt. These findings are consistent with a six-fold coordinated iron in the solid and a four-fold coordinated iron in the solution/quick-frozen solutions.

The breadth of the XANES spectra is determined by the energy resolution of the beamline. The monochromator band pass is between 1.5–2 eV at the Fe K edge and together with a core hole width of 1.25 eV this results in about 2.15 eV resolution. Nuclear vibration amplitudes at room temperature are of the order of 0.1 \AA ,⁴⁶ so line broadening of the order of a few tenths of an eV will result, this being small compared to the 2 eV breadth from other cumulative causes. The fine structure of the pre-edge is nevertheless observable and further confirms the difference in coordination for the solid and for the solutions (both native and quick-frozen).

The combined use of ligand field theory and DFT calculations⁴⁸ has demonstrated that the width reflects the ligand field splitting of the 3d in different geometries.

In the high-spin ferric d^5 in octahedral geometry, the $^5A_{1g}$ ground state has a $(t_{2g})^3(e_g)^2$ configuration. Promotion of a 1s electron into the 3d manifold produces 2 excited configurations

$(t_{2g})^2(e_g)^2$ and $(t_{2g})^3(e_g)^1$ and coupling of the holes in these configurations give the 5T_2 and 5E states, respectively. As a result, the pre-edge appears to split. The energy separation of the two features can be related to ligand strength, and their approximate electric quadrupole intensity ratio should be 3 : 2, with any deviations reflecting differences in covalency. For the solid sample, the $1s \rightarrow 3d$ pre-edge peak has been fitted with two pseudo-Voigt functions, following the procedure described in the literature.⁴⁸ The difference in peak energy (1.59 eV) and the ratio between their intensities (0.56) are within the interval found for high-spin octahedral ferric complexes described in Table 1 of ref. 48

For a tetrahedral geometry, there are two one-electron allowed excited hole configurations $(t_2)^2(e)^2$ and $(t_2)^3(e)^1$ that produce a triply degenerate 5T_2 and a doubly degenerate 5E . The $4p$ orbital transforms as t_2 so that only mixing into the $3d$ t_2 set contributes to the intensity of the transition to the 5T_2 state. Such an assignment could hold for the solution as seen in Fig. 5, but the case of quick-frozen solutions is clearly more complex.

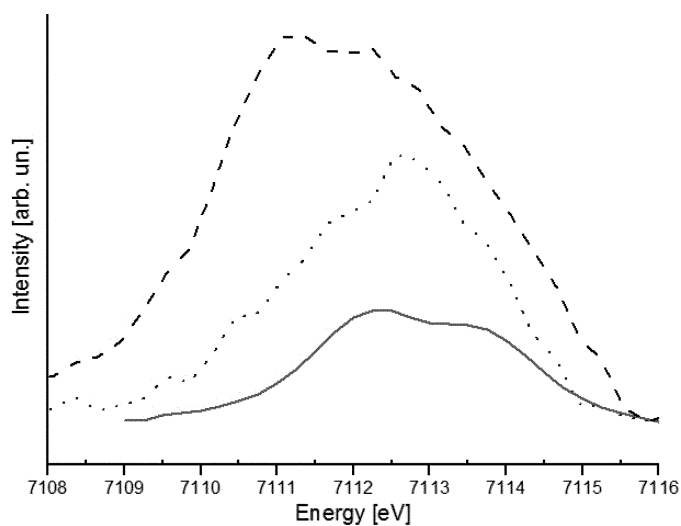


Fig. 5 Pre-edge spectra of the solid ferric-hydroxo complex salt (lower spectrum), the strongly alkaline ($[NaOH]_T = 20$ M) solution supersaturated with ferric ions (upper spectrum) and the same supersaturated solution after quick-freezing (middle spectrum).

When considering the other spectral regions, the edge and edge crest are systematically shifted towards lower energy for the solution samples as shown in Fig. 5. The amplitude of the crest edge decreases and the slope within the peak changes.⁴⁰ The differences are clearly seen in the derivative XANES spectra for the solid, solution and frozen solution (Figure S2 in the ESI†). The breadth is the largest for the frozen solution sample due to a shoulder at the energy expected for the $1s \rightarrow 4s$ transition. The shift by about 2 eV⁴⁰ can be related to a decrease in the effective ionic charge of the metal,⁴⁰ since the binding energy of the $1s$ electron decreases with a decreasing number of nearest neighbours. All these findings corroborate with a lower coordination number of iron in solution than in solid.

EXAFS spectra. Analysis by mathematical refinement of the phases, amplitudes and frequencies of the EXAFS structure function was performed by using the EXCURVE software package to obtain accurate interatomic distances and estimates of

coordination numbers of the Fe(III) in the solid sample and in the quick-frozen solution. Models were rejected on the basis of high residuals. The data used during the refinements included the raw radial distribution function distances, empirically determined phase shift corrections (+0.64 for Fe and +0.56 for O) and expected bond lengths for possible metal–ligand pairs as a function of oxidation state and coordination number.

For the central Fe, the $Z + 1$ core hole approximation was chosen. A value of 1 was chosen for the amplitude reduction factor. Curve fitting of the k^3 -weighted fine structure was done on the raw data. The best fit was searched by minimization of the fit index defined as the sum of the residuals squared divided by the number of data points.

The structural parameters extracted from the EXAFS analysis (in accordance with the conclusions from the XANES) strongly support the presence of an octahedrally coordinated complex in the solid sample. When the structural function was fitted with six Fe–O contributions, $r_{Fe-O} = 2.036$ – 2.040 Å and a Debye–Waller factor of 0.015 gave the best fit.

Although the general shape of the fitted line matches well with the experimental data, the fitting factor was found to be unsatisfactory. Therefore a model with two additional iron ($r_{Fe-Fe} = 3.51$ Å) and two sodium ($r_{Fe-Na} = 3.27$ – 3.29 Å) atoms was tested. This caused a significant improvement in the fit (Fig. 6a), but left the r_{Fe-O} distance (2.030 Å) and the Debye–Waller factor (0.015) unaltered. From this observation, it seems that the contribution of additional heavy metals is significant in determining the shape of the EXAFS structure function.

To fit the EXAFS spectrum of the frozen-liquid sample, guided by the XANES results, a tetrahedral model was used. The general shape was satisfactorily reproduced (Fig. 6b), but unfortunately the unfavourable signal-to-noise level did not allow for obtaining a very good fitting factor in this case. The r_{Fe-O} values were found to be in the range of 1.86– 2.01 Å, consistent with the first neighbour interatomic distances for oxygen coordinated ferric ions in a tetrahedral environment (1.8– 1.9 Å⁴¹).

Values for the bond distances can be checked vs. the coordination number using valence bond sum analysis,⁴⁹ where the bond valence is expressed as: $s_{ij} = \exp[(R_{ij} - d_{ij})/b]$, where d_{ij} is the distance between atom i and j , R_{ij} is the empirically determined distance and b is generally set to 0.37. Values of R_{ij} that give bond valence sums near the oxidation state have been tabulated.^{50–52}

Conclusion

From strongly alkaline aqueous solutions, a solid ferric-hydroxo complex salt has been isolated. Mössbauer spectroscopic data proved that the environment of iron is highly symmetrical and from XANES and EXAFS measurements it has been demonstrated, that the coordination number of the ferric ion is six, with a primary Fe–O bond distance of 2.03 Å. Thus, the elementary building block of the solid complex is $[Fe(OH)_6]^{3-}$. The structure of the ferric ions in solutions, from which the solid hydroxo complex salt has been isolated, was found to be markedly different from that of the solid compound. Both the EXAFS and XANES data suggest, that in solution the highest coordination number stepwise ferric-hydroxo complex formed is the tetrahedral $[Fe(OH)_4]^-$. To the best of our knowledge, our work is the first direct structural observation, which unequivocally proves that ferric-hydroxo complexes with

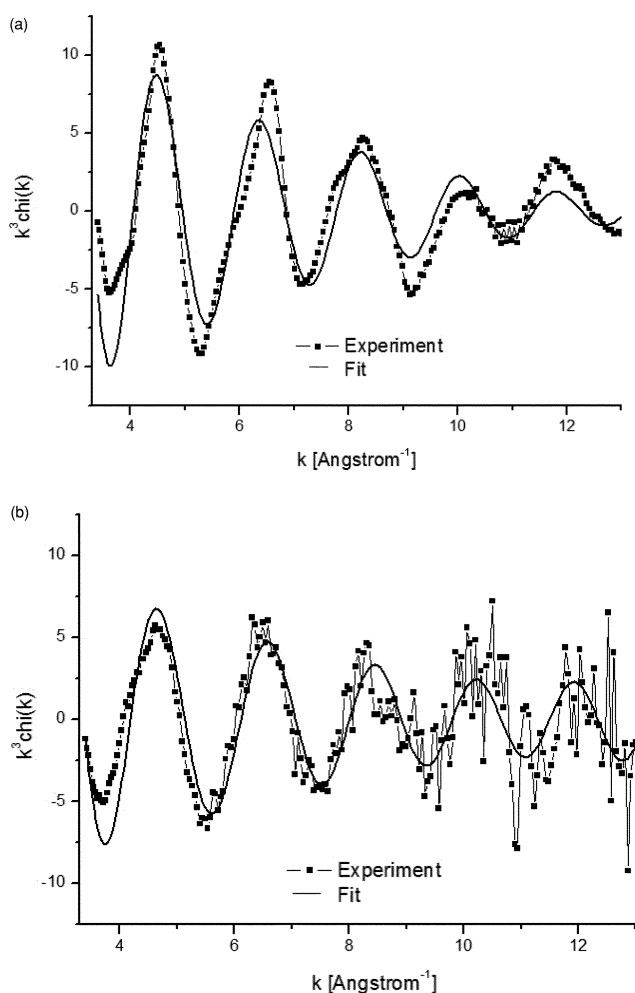


Fig. 6 EXAFS spectra of the solid ferric-hydroxo complex salt (a) and that of the quick-frozen strongly alkaline ($[\text{NaOH}]_{\text{T}} = 20 \text{ M}$) solution supersaturated with ferric ions (b). The solid lines represent the fitted curves without the contribution from the second coordination shell.

more than 4 hydroxide ions do not form in experimentally observable quantities in aqueous solution even at the highest possible base concentrations. On this count, the behaviour of Fe(III) is very similar to that of Al(III) and Ga(III).

Acknowledgements

The authors would like to express their gratitude to Dr Ottó Berkesi (for recording and interpreting the IR and Raman spectra), to Dr Ágnes Hemmert-Patzkó (for determining the XRD patterns), to Mrs Katalin Barna (for the TG/DTG measurements) to Mrs Katalin Szűcs (for assisting with the pH-potentiometric measurements) and to Dr Katharina Norén and Dr Stefan Carlson (for their assistance in recording the XANES/EXAFS spectra). The research was supported by grants of the Hungarian Science Foundation (OTKA K62691, K68135 and K67835) and by the TARI Grant from MaxLab (Experiment No. I811-072).

References

1 T. W. Swaddle, J. Rosenquist, P. Yu, E. Bylaska, B. L. Philips and W. H. Casey, *Science*, 2005, **308**, 1450.

- 2 K. L. Shafran and C. C. Perry, *Dalton Trans.*, 2005, 2098.
- 3 M. R. Anseau, J. P. Leung, N. Sahal and T. Swaddle, *Inorg. Chem.*, 2005, **44**, 8023.
- 4 (a) P. Sipos, G. T. Hefter and P. M. May, *Dalton Trans.*, 2006, 368; (b) P. Sipos, M. Schibecchi, G. Peintler, G. T. Hefter and P. M. May, *Dalton Trans.*, 2006, 1858.
- 5 P. Sipos, O. Berkesi and T. Megyes, *J. Soln. Chem.*, DOI: 10.1007/s10953-008-9314-y.
- 6 T. Radnai, P. M. May, G. T. Hefter and P. Sipos, *J. Phys. Chem. A*, 1998, **102**, 7841.
- 7 K. R. Bauspiess, T. Murata, G. Parkinson, P. Sipos and H. Watling, *J. Phys. IV*, 1997, **7**, 485.
- 8 P. Sipos, G. T. Hefter and P. M. May, *Talanta*, 2006, **70**, 761.
- 9 C. F. Baes, R. E. Mesmer, *The Hydrolysis of Cations*, Wiley, New York, 1976, p. 237.
- 10 A. A. Kamnev, B. B. Ezhov and O. G. Malandin, *USSR Koord. Khim.*, 1988, **14**, 25.
- 11 A. A. Kamnev and B. B. Ezhov, *Koord. Khim.*, 1990, **16**, 1650.
- 12 X. Liu and F. J. Millero, *Geochim. Cosmochim. Acta*, 1999, **63**, 3487.
- 13 I. I. Diakonov, J. Schott, F. Martin, J.-C. Harrychourry and J. Escalier, *Geochim. Cosmochim. Acta*, 1999, **63**, 2247.
- 14 R. H. Byrne, Y.-R. Luo and R. W. Young, *Mar. Chem.*, 2000, **70**, 23.
- 15 F. A. Cotton, G. Wilkinson, *Advanced Inorganic Chemistry*, Wiley, New York, 3rd edn, 1972, p. 712.
- 16 W. N. Perera and G. Hefter, *Inorg. Chem.*, 2003, **42**, 5917.
- 17 M. Pasero, N. Perchiazzi, S. Bigi and S. Merlino, *Eur. J. Mineral.*, 1997, **9**, 43.
- 18 G. S. Li, Y. C. Mao, X. R. Li, L. J. Zhu and S. H. Feng, *Chem. J. Chin. Univ.*, 1998, **19**, 1195.
- 19 D. Y. Pushcharovsky, Y. S. Lebedeva, N. V. Zubkova, M. Pasero, M. Bellezza, S. Merlino and N. V. Chukanov, *Can. Mineral.*, 2004, **42**, 723.
- 20 R. Scholder, *Angew. Chem.*, 1953, **65**, 240.
- 21 R. Scholder and E. F. Schwochow, *Angew. Chem., Int. Ed. Engl.*, 1966, **5**, 1047.
- 22 R. Scholder, in *Handbook of Preparative Inorganic Chemistry*, ed. G. Brauer, Academic Press, New York, London, 2nd edn., 1965, vol. 2, part III, section 2, p. 1688.
- 23 J. Burgess, in *Comprehensive Coordination Chemistry*, ed. G. Wilkinson, R. D. Gillard and J. A. McCleverty, Pergamon, Oxford, 1987, vol. 2, p. 305.
- 24 H. R. Watling, P. Sipos, L. Byrne, G. T. Hefter and P. M. May, *Appl. Spectrosc.*, 1999, **53**, 415.
- 25 V. Zabel, M. Schneider, M. Weinberger and W. Gessner, *Acta Crystallogr., Sect. C: Cryst. Struct. Commun.*, 1996, **52**, 747.
- 26 M. Loeper, M. Schneider, W. Gessner and G. Reck, *Z. Kristallogr.*, 1996, **211**, 709.
- 27 A. A. Kamnev, B. E. Ezhov, N. S. Kopelev, Y. M. Kiselev and Y. D. Perflyev, *Electrochim. Acta*, 1991, **36**, 1253.
- 28 A. A. Kamnev, B. E. Ezhov, V. Rusanov and V. Angelov, *Electrochim. Acta*, 1992, **37**, 469.
- 29 A. A. Kamnev, Y. D. Perflyev and V. Angelov, *Electrochim. Acta*, 1995, **40**, 1005.
- 30 P. Sipos, G. T. Hefter and P. M. May, *Analyst*, 2000, **129**, 955.
- 31 N. Balázs and P. Sipos, *Carbohydr. Res.*, 2007, **342**, 124.
- 32 Z. Klencsár, E. Kuzmann and A. Vértes, *J. Radioanal. Nucl. Chem.*, 1996, **210**, 105.
- 33 S. Carlson, M. Clausen, L. Gridneva, B. Sommarin and C. Svensson, *J. Synchrotron Radiat.*, 2006, **13**, 359.
- 34 U. Schwertmann, R. Cornelle, *Iron Oxides in the Laboratory*, VCH Verlagsgesellschaft mbH, Weinheim, 1991.
- 35 P. Sipos, P. M. May, G. T. Hefter and I. Kron, *J. Chem. Soc., Chem. Commun.*, 1994, 2355.
- 36 K. Nakamoto, *IR and Raman Spectra of Inorganic and Coordination Compounds*, Wiley-Interscience Publications, New York, USA, 1997.
- 37 J. Chappert, R. B. Frankel, A. Misetich and N. A. Blum, *Phys. Rev.*, 1969, **179**, 578.
- 38 A. Vértes, L. Korecz, K. Burger, *Mössbauer spectroscopy*. Elsevier, Lausanne, Switzerland, 1979.
- 39 A. Vértes, D. L. Nagy, *Mössbauer spectroscopy of frozen solutions*. Akadémiai Kiadó, Budapest, Hungary, 1990.
- 40 W. Liu, B. Etschmann, J. Brugger, L. Spiccia, G. Foran and B. McInnes, *Chem. Geol.*, 2006, **231**, 326.
- 41 M. J. Afted, G. A. Waychunas and G. E. Brown, *Geochim. Cosmochim. Acta*, 1985, **49**, 2081.

- 42 G. A. Waychunas, M. J. Apter and G. E. Brown, Jr., *Phys. Chem. Miner.*, 1983, **10**, 1.
- 43 M. Wilke, F. Farges, P. E. Petit, G. E. Brown and F. Martin, *Am. Mineral.*, 2001, **86**, 714.
- 44 A. J. Berry, H. S. C. O'Neill, K. D. Jayasuriya, S. J. Campbell and G. J. Foran, *Am. Mineral.*, 2003, **88**, 326.
- 45 R. G. Schulman, Y. Yafet, P. Eisenberger and W. E. Blumberg, *Proc. Natl. Acad. Sci. U. S. A.*, 1976, **73**, 1384.
- 46 G. Mitchell and W. W. Beeman, *J. Chem. Phys.*, 1952, **20**, 1298.
- 47 A. L. Roe, D. J. Schneider, R. J. Mayer, J. W. Pyrz, J. Widom and L. Que, Jr., *J. Am. Chem. Soc.*, 1984, **106**, 1676.
- 48 T. E. Westre, P. Kennepohl, J. G. DeWitt, B. Hedman, K. O. Hodgson and E. I. Solomon, *J. Am. Chem. Soc.*, 1997, **119**, 6297.
- 49 I. D. Brown, *The Chemical Bond in Inorganic Chemistry: The Bond Valence Model*, Oxford University Press, New York, 2002.
- 50 I. D. Brown and D. Altermatt, *Acta Crystallogr., Sect. B: Struct. Sci.*, 1985, **41**, 244.
- 51 N. E. Brese and M. O'Keefe, *Acta Crystallogr., Sect. B: Struct. Sci.*, 1991, **47**, 192.
- 52 M. O'Keefe, *Acta Crystallogr., Sect. A: Found. Crystallogr.*, 1990, **46**, 138.